Development 140, 405-412 (2013) doi:10.1242/dev.085787

The *Liguleless narrow* mutation affects proximal-distal signaling and leaf growth

Jihyun Moon[1], Héctor Candela[2] and Sarah Hake[1,3,*]

SUMMARY

How cells acquire competence to differentiate according to position is an essential question in developmental biology. Maize leaves provide a unique opportunity to study positional information. In the developing leaf primordium, a line is drawn across a field of seemingly identical cells. Above the line, the cells become blade, below the line the cells become sheath and at the line, the cells differentiate into the specialized tissues of ligule and auricle. We identified a new mutation, *Liguleless narrow* (*Lgn*), that affects this patterning and shows striking defects in lateral growth as well, thus linking proximal-distal patterning to medial-lateral growth. In characterizing the defect we discovered that both the auxin transport protein ZmPIN1a and the squamosa promoter-binding protein LIGULELESS1 are expressed precisely at this positionally cued line and are disrupted by *Lgn*. Positional cloning and a transposon-derived allele demonstrate that LGN is a kinase. These results suggest that LGN participates in setting up positional information through a signaling cascade. Interestingly, LGN has a paralog that is upregulated in the mutant, suggesting an important feedback mechanism involved in setting the positional boundary.

KEY WORDS: PIN1, Leaf development, Maize, Pattern establishment, Preligule

INTRODUCTION

Leaves continuously develop at the flanks of an active shoot apical meristem, where a population of pluripotent stem cells resides. Starting as a bulge on the flank of the meristem, the newly initiated leaf becomes asymmetric in several axes: adaxial-abaxial, medial-lateral and proximal-distal. Polarization along these axes leads to the asymmetric distribution of cell types in the mature organ (Eshed et al., 2001; Moon and Hake, 2011). Maize serves as an excellent model system for the study of leaf development due to the well-organized pattern of division during leaf development and the distinct tissue types in the mature leaf (Fig. 1A). Along the proximal-distal axis, the sheath is proximal, the blade is distal and a ligular region, which consists of the ligule and auricle, is at the blade-sheath boundary. The midrib and margins of each leaf constitute the medial-lateral axis. Adaxial and abaxial epidermal surfaces have different distributions of cell types. Mutations affecting one or more of the developmental axes disrupt the patterning of the leaf, leading to a change in cell identity at specific regions.

The ligule is an adaxial structure found at the blade-sheath boundary of most grass leaves. The main function of a ligule is to repel water from entering the space between the leaf sheath and stem, where axillary buds form. Two recessive mutants, *liguleless1* (*lg1*) and *lg2*, provide important information in deciphering the genetic basis of leaf patterning in maize (Becraft and Freeling, 1991; Becraft et al., 1990; Harper and Freeling, 1996; Moreno et al., 1997; Sylvester et al., 1990; Walsh et al., 1998). The *lg1-R* mutation removes the ligule and auricle from most of the leaves, but the blade-sheath boundary remains distinct (Sylvester et al., 1990). *lg2-R* mutants lack ligules and auricles only on the first initiated leaves. In later-formed leaves, ligule and auricle appear at both leaf margins but the position is displaced relative to one another. *lg1* encodes a squamosa promoter-binding protein that is expressed at the ligular region (Moreno et al., 1997). *lg2* encodes a basic leucine zipper protein (bZIP) and its mRNA is expressed more broadly (Walsh et al., 1998). Mosaic analysis has shown that the *lg1-R* phenotype is cell autonomous whereas *lg2-R* is non-cell-autonomous (Becraft and Freeling, 1991; Harper and Freeling, 1996; Moreno et al., 1997). These results together lead to a proposal that LG2 acts by regulating the 'make ligule/auricle' signal, whereas LG1 might be involved in reception and/or downstream signal transduction of the signal (Walsh et al., 1998).

Here, we describe the characterization and cloning of the semi-dominant *Liguleless narrow-Reference* (*Lgn-R*) mutant. In *Lgn-R* heterozygotes, mRNA levels of *lg1* and *lg2* are reduced and boundary formation fails towards the margins of the leaf. Leaves are narrow and branching in the inflorescence is reduced, suggesting a link between proximal-distal patterning and lateral growth. Homozygous *Lgn-R* plants fail to produce reproductive structures and remain in a juvenile state. We mapped *Lgn* to a kinase and showed that the *Lgn-R* mutation results in decreased kinase activity and increased mRNA levels of its paralog, *sister of liguleless narrow* (*sln*). Together, these results suggest that the regulation *of lgn* and *sln* is crucial for establishing positional cues that have major impacts on developmental processes.

MATERIALS AND METHODS

Plant materials

Lgn-R was found in an ethyl methanesulfonate (EMS) M1 screen in the B73 background performed by M. G. Neuffer (University of Missouri, Columbia). The chimera plant was crossed to A632, then introgressed five to six generations into inbreds including B73, W22 and W23. The *tac905.29* allele is an *Ac* insertion line generated by the Dooner laboratory (Cowperthwaite et al., 2002). Seeds (Co-op ID: T3211H) were obtained from the Maize Genetics Cooperation Stock Center (http://maizecoop.cropsci.uiuc.edu/). *lg1-R* in W23 background was used

[1]Department of Plant and Microbial Biology, University of California, Berkeley, CA 94720, USA. [2]Instituto de Bioingeniería, Universidad Miguel Hernández, Campus de Elche, 03202 Elche, Alicante, Spain. [3]Plant Gene Expression Center, United States Department of Agriculture-Agriculture Research Service and the University of California, Albany, CA 94710, USA.

*Author for correspondence (hake@berkeley.edu)

Accepted 8 November 2012

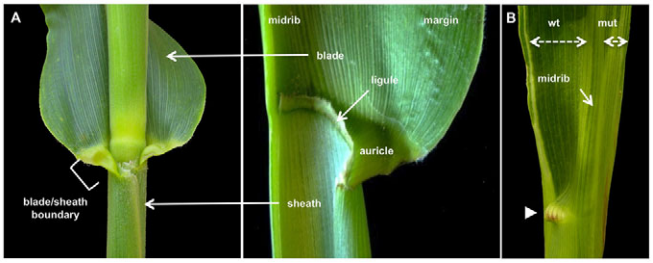

Fig. 1. Maize leaf structure and the *Lgn-R* half-plant chimera. (**A**) The maize leaf consists of four distinct tissue types along the proximal-distal axis with the blade positioned distal to the sheath. The ligule and auricle are at the boundary between blade and sheath. Position of the midrib and margin is shown on a leaf cut along the midrib (right). (**B**) Leaf of the original *Lgn-R* half-plant chimera. One half of the leaf is narrow with a defective blade-sheath boundary (arrowhead). The other half is wider and its margin lacks auricle and ligule owing to the fact that maize leaves initiate as encircling rings.

to generate *lg1-R Lgn-R/+* and for qRT-PCR analysis. *lg2-R* is in an undefined background. ZmPIN1a-YFP lines have been described previously (Gallavotti et al., 2008).

Plant measurements

All measurements were done on the sixth leaf counting down from the top after the tassel had emerged. Ten plants were measured per genotype. The numbers were averaged and standard deviation was calculated. Blade length was measured along the midrib from the ligule to the tip and blade width was measured across the half-point of the leaf between the blade tip and ligule region. The whole-plant height was measured from the ground to the highest node beneath the tassel.

Epidermal surface replicate

Epidermal surface of the leaves were observed by the modified replica technique (Foster et al., 2004). Casts of epidermal surfaces were generated by applying dental impression medium to the leaf surface. Colorless nail polish was applied to the cast and left to dry overnight. Dried nail polish replicas were peeled off from the cast and placed on a microscope slide with water. Coverslips were mounted and the specimens were viewed under a Zeiss Axiophot differential interference contrast (DIC) microscope.

Positional cloning of *lgn*

F1 plants of *Lgn-R* in B73 crossed to selected inbreds (Mo17, A632 and W22) were backcrossed to that inbred to generate mapping populations. Genetic linkage of *Lgn-R* to chromosome 9 was first detected by bulked segregant analysis (Michelmore et al., 1991) using simple sequence repeat (SSR) markers on different maize chromosomes. Fine mapping was carried out using genomic DNA from 2800 segregating plants. Information on the SSR markers used is available from MaizeGDB (http://www.maizegdb.org). Additional single nucleotide polymorphisms (SNP) markers were designed based on genes syntenic to the rice genome in the region. Among the ~80 genes in the region, cDNA of 24 candidate genes were sequenced. The coding region and the 5′UTR of the candidate gene were sequenced in *Lgn-R*, *tac905.29* and *Lgn-dAc*.

Whole-genome sequencing

Leaves from 700 homozygous *Lgn-R* F2 plants of a *Lgn-R* (B73)/Mo17 mapping population were pooled. Genomic DNA libraries were prepared according to the standard Illumina protocol using Illumina PE adapters and oligonucleotides, and other reagents were obtained from major manufacturers (Promega, NEB). Nuclei were isolated from the pooled leaves as previously described (Schmidt et al., 1992), chromatin was sheared using Covaris to obtain an average size of ~300 bp. After end repairs, A-tailing and ligation of adapters, gel selection was carried out for a size of 400 bp and was followed by a PCR amplification of ten cycles. Libraries were sequenced (100 bp, paired-ends) on an Illumina HiSeq 2000 at Vincent J. Coates Genomics Sequencing Laboratory (University of California Berkeley, CA, USA). The reads were aligned to a hard-masked version (with the repeats replaced by Ns) of the genomic sequence of chromosome 9 by Bowtie software (Langmead et al., 2009), which was run using SHORE's mapflowcell option (Ossowski et al., 2008), allowing the alignment of reads with up to two mismatched nucleotides. The resulting file was processed using SHORE's correct4pe option to remove incorrectly aligned reads based on the position of paired-end reads. The output of this program (in map.list format) was converted to Sequence Alignment/Map (SAM) format using SHORE's convert option, and then to BAM format using the SAMtools package (Li et al., 2009). The resulting BAM file was processed with the SAMtools mpileup and bcftools commands to prepare a list of mutations and polymorphisms in the candidate interval, which was finally examined using the Integrative Genomics Viewer (IGV) (Robinson et al., 2011) to check for G/C to A/T mutations.

RNA isolation and expression analysis

Total RNA was purified using Trizol reagent according to the manufacturer's instructions (Invitrogen). RNA (1 μg) from each sample was reverse-transcribed using Superscript (Invitrogen). Quantitative PCR was performed on a MyIQ single-color real-time detection system (Bio-Rad) and data were processed in MyIQ and Excel. Data are from at least three qPCR replicates and were normalized against *gapdh* levels. Primers used are as follows: *gapdh*, ZmGAPDH-5F, 5′-CCTGCTTCTCATGGATGGTT-3′ and ZmGAPDH-6R, 5′-TGGTAGCAGGAAGGGAAACA-3′; *lgn*, JM89F, 5′-CACCATCCGGAGATCCCT-3′ and JM89R, 5′-TTGTTGGCCTTGGAGAAGTT-3′; *sln*, JM85F, 5′-ATGGAGGAACAACACATGGC-3′ and JM85R, 5′-GATAGACGGGCCCGAAACCG-3′; *lg1*, lg1-3′F, 5′-GCTAAAGACAAAGCAGAGAG-3′ and lg1-3′R, 5′-CTAGTGATCGAAGTCGAGATC-3′; *lg2*, lg2-3′F, 5′-GGAAGCTCTCGCCCAGGGCC-3′ and lg2-3′R, 5′-TCAAAATCCGGCGAACTGG-3′. For semi-quantitative RT-PCR, same primers were used for *sln* and JM95F 5′-CTGCAGGTGCTGACAAGGAC-3′ was used with JM89R for *lgn*.

Whole-mount *in situ* hybridization

The antisense *lg1* probe (same primers as above) was generated by using the 3′ end of the *lg1* cDNA as a template. *In vitro* transcription was carried out with T7 RNA polymerase (Promega) using DIG RNA Labeling Mix (Roche). Whole-mount *in situ* hybridization was performed as previously described (Chuck et al., 2002) with the following modifications. Immature leaves were dissected and fixed in 3.7% formaldehyde, 5% acetic acid, 50% ethanol (FAA) (+ 1% Triton X-100, 1% DMSO) for 2 hours with rotation at room temperature. Pre-hybridization was carried out overnight at 55°C before adding the probes to the hybridization solution (6× SSC, 3% SDS, 50% formamide, 100 μg/ml tRNA). To avoid the floating of tissue, Triton X-100 was added to the washes when needed.

Phylogenetic analysis

Alignments of predicted full-length amino acid sequences were carried out automatically using MUSCLE software (Edgar, 2004). The phylogenetic tree was constructed based on the alignment using Phylogeny.fr (Dereeper et al., 2008).

Autophosphorylation assay

In order to express the kinase domain of the wild-type and mutant forms of LGN, *lgn* cDNA corresponding to the kinase domain was amplified and cloned into *pGEX-5X-2* (GE Life Sciences). For the kinase domain amplification, JM77F, 5′-CCCGGATCCCGGTCGAGCTCGGACCTGCCG-3′ and JM77R, 5′-CCCGAATTCTCATCGCGGTTCGATCATGG-3′ were used.

Bacteria transformed with wild-type and mutant GST::LGNΔTMD constructs were induced for 2 hours with 1 mM isopropylthio-β-galactoside (IPTG) when OD_{600} was 0.5 to 0.7. The bacterial pellet was collected by centrifugation and lysed using Cell-Lytic B Reagent (Sigma). The soluble fraction (1 ml) was added to 200 μl of a slurry of Glutathione agarose beads (Sigma) pre-equilibrated in Cell-Lytic B and 1% Triton X-100, and tubes were rocked for 1 hour at 4°C. Beads were washed three times. For kinase assays, 10 μl of glutathione beads containing the bound protein were mixed with 4 μl 5×kinase buffer (125 mM Tris, pH 7.5, 25 mM $MgCl_2$, 1

mM EDTA), 1 μl [γ-^{32}P]ATP (specific concentration 3000 Ci/mM) and 4.8 μl dH_2O, and incubated for 30 minutes at 30°C. One volume of SDS-PAGE loading buffer (250 mM Tris-HCl pH 6.8, 2% SDS, 30% glycerol, 0.1 M DTT, 0.02% Bromophenol Blue) was added to each sample. Samples were boiled and spun briefly, and 15 μl of the supernatant was separated on 12% polyacrylamide gels.

RESULTS

The dominant *Lgn-R* mutation affects leaf patterning and inflorescence development

Lgn-R was isolated as an M1 half-plant chimera following EMS mutagenesis of pollen from the B73 inbred background. In an EMS-induced chimera, half the plant carries the mutation whereas the other half does not (Candela and Hake, 2008; Neuffer et al., 2009). One half of the *Lgn-R* chimera appeared narrow with a missing ligule region whereas the other half of the leaf had expanded to near normal width and had some auricle tissue (Fig. 1B, arrowhead). The sector of mutant tissue included one entire half of a leaf and the margin of the other half. The mutation in the half-plant chimera was introgressed into different maize inbred backgrounds for further characterization. Analyses presented here were carried out in the B73 inbred background unless otherwise specified. *Lgn-R* heterozygotes are shorter in height and display reduction in leaf width and length (Fig. 2A-C; Table 1). Reproductive development is also affected in the mutant. The tassel, which is the terminal inflorescence, has fewer branches (Fig. 2D; Table 1), and the ears, which are inflorescence branches from the main shoot, frequently fail to form. The phenotype is more severe as a homozygote; the height is <30 cm and plants fail to produce any reproductive organs (Fig. 2A).

Blade morphology is moderately affected in *Lgn-R* whereas the sheath is relatively unaffected. Supernumerary epidermal hairs appear on the adaxial surface of the blade and, occasionally, ectopic abaxial hairs occur (Fig. 2E,F). The normal pattern of vasculature, however, suggests that the ectopic abaxial hair is not due to adaxial-abaxial polarity defects. The epidermal cellular morphology of the blade (Fig. 2G,J) and sheath (Fig. 2H,K) appears similar in wild type and *Lgn-R*. The most significant defect of *Lgn-R* leaves is found at the blade-sheath boundary, where auricles and ligule normally develop. In *Lgn-R*, these tissues are greatly reduced, with just a patch of ligule near the midrib (Fig. 2B,C). At the margins of *Lgn-R* leaves, sheath tissue extends into the blade or blade into sheath (supplementary material Fig. S1). Isolated patches of auricle cells are found intermixed between sheath cells (Fig. 2L) compared with the well-defined area of auricle cells in wild-type leaves (Fig. 2I). These results suggest that *lgn* might function in establishment of the blade-sheath boundary during leaf development.

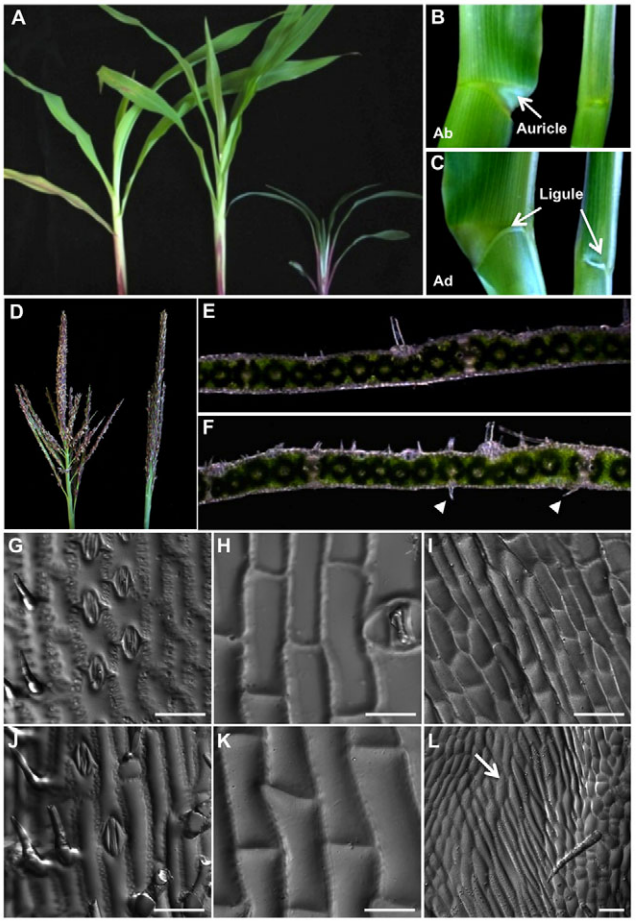

Fig. 2. Phenotype of *Lgn-R*. (**A**) Two-week-old seedling phenotype of wild-type, *Lgn-R* heterozygous and homozygous maize, from left to right. (**B**) Abaxial surface of the mature wild-type (left) and *Lgn-R*/+ (right) leaf. The auricle is greatly reduced in the mutant. The midrib is towards the left. (**C**) Adaxial surface of the leaves shown in B. A patch of ligule appears near the midrib but fails to extend towards the margin in *Lgn-R*/+. The midrib is to the right. (**D**) Tassel branch number is reduced in *Lgn-R*/+ (right) compared with wild type (left). Tassel branches are also more upright. (**E**,**F**) Cross section of blade in wild type (E) and *Lgn-R*/+ (F). Adaxial surfaces face upward. *Lgn-R*/+ leaf has ectopic hairs on the abaxial surface (arrowheads). (**G-L**) Adaxial epidermal surface replicates of wild type (G-I) and *Lgn-R*/+ (J-L). Blade (G,J) and sheath (H,K) cells are similar whereas the auricle cells (I) are intermixed with different cell types in *Lgn-R*/+ (marked with white arrow) (L). Scale bars: 100 μm.

The preligule band is not elaborated in *Lgn-R*

Preligular development, which occurs very early in leaf development, leads to differentiation of the ligule and auricle. In leaves that are the fifth to seventh from the meristem (P5-7), a horizontal band of small cells derived by both longitudinal and transverse anticlinal divisions appears along the epidermal surface (Fig. 3A-C). Following these rapid anticlinal divisions, periclinal divisions initiate and generate a ridge of cells growing out from the surface of the leaf, which will eventually form the ligule. We discovered that this process can be imaged by localizing the auxin efflux transporter, maize PINFORMED 1a (ZmPIN1a) by a YFP fusion (Carraro et al., 2006; Gallavotti et al., 2008; Gälweiler et al., 1998). As expected, ZmPIN1a was found expressed at high levels in lateral and intermediate veins (Fig. 3D) and the subcellular localization was towards the basal membrane of the cell. ZmPIN1a was also observed in the epidermal cells forming the preligule band (Fig. 3D-G). Interestingly, ZmPIN1a in these cells showed polarized localization towards the lateral membranes, suggesting a flow of auxin along the medial-lateral axis within the developing preligule band (supplementary material Fig. S2). The position of the preligular band coincides with the zone of intermediate vein anastomosis (Fig. 3E, arrowhead), indicating that an earlier signal exists to mark the position where the blade-sheath boundary will form.

Lgn-R leaves showed defects starting at P5. Small epidermal cells resulting from anticlinal divisions were observed, indicating that cells had initiated divisions (Fig. 3H,I). The small cells,

Table 1. Measurement of *Lgn-R* phenotype in B73 and W22

	Width (cm)	Length (cm)	Height (cm)	Tassel branch*
B73	8.29±0.48	65.14±3.44	169.40±2.51	10.00±1.22
Lgn-R/+	3.57±0.61	38.43±4.47	115.25±16.26	5.60±0.89
W22	11.92±1.78	64.4±1.75	115.20±4.55	14.33±4.17
Lgn-R/+	6.02±0.99	46.6±1.71	91.80±10.21	5.37±1.85

*Number of lateral branches was counted.
n=20 for all measurements.

however, never formed a continuous band, but rather appeared in an erratic manner. Later-stage leaves showed some periclinal divisions that resulted in outgrowth of ligular patches near the midrib, but a continuous preligular band was never observed (Fig. 3J). Similarly, epidermal ZmPIN1a localization was found in some cells but not in a continuous band (Fig. 3K,L). The localization appeared only near the midrib where the ligular patches develop. These results suggest that the defect observed in *Lgn-R* begins prior to preligular band formation, at an early stage of leaf development when the boundary zone forms.

Lgn-R and the *liguleless* mutants function in the same pathway

In order to determine the effect of the *Lgn-R* mutation on *lg1* and *lg2* expression, different domains were harvested from developing leaves: the preligular band of P5-7 leaves, immature blade of P5-7 leaves and the shoot apex including P0-4 leaves. Our qRT-PCR analysis on these dissected tissues agrees with the previous studies (Moreno et al., 1997; Walsh et al., 1998) showing that in normal leaves, *lg1* accumulation occurs mainly at the preligular band region, whereas *lg2* has a broader expression pattern throughout the developing leaf (Fig. 4A). In *Lgn-R* leaves, both *lg1* (P=0.046) and *lg2* (P=0.026) mRNA accumulation levels were decreased at the preligular domain (Fig. 4A). *lg2* mRNA levels were also significantly decreased in the shoot apex (P=0.0091) of *Lgn-R*/+. Previous attempts to localize the *lg1* mRNA on sectioned material were not successful (Moreno et al., 1997). Thus, considering the restricted domain of expression, we carried out whole-mount *in situ* hybridization. *lg1* was expressed in a narrow band near the base of an immature normal leaf and was absent in the *lg1-R* mutant (Fig. 4B), which is consistent with the qRT-PCR analysis. In *Lgn-R*, *lg1* expression was found only near the midrib where patches of ligules form, suggesting that *lg1* expression correlates with the occurrence of the ligule (Fig. 4B).

lg1-R mutant leaves lack all ligule and auricle, but the blade-sheath boundary is well defined (Fig. 4C), unlike *Lgn-R*, which lacks a sharp boundary at the margin of the leaf (Fig. 2B,C). In order to understand the genetic interaction between *lg1-R* and *Lgn-R*, a double mutant was generated. As *lg1-R* was in a W23 inbred background, the subsequent analysis was carried out with *Lgn-R* introgressed into W23. *Lgn-R* heterozygotes show a milder phenotype in W23 compared with that in B73; the ligule occasionally extends completely to the margin and auricles are reduced rather than absent (Fig. 4C). The plants, however, are still short and the leaves are shorter and narrower. Addition of the *lg1-R* mutation to *Lgn-R* enhances the boundary defect of *Lgn-R* such that the ligule/auricle and the blade-sheath boundary fail to form altogether (Fig. 4C). This phenotype is more severe than each single mutant, suggesting a synergistic interaction between the two mutations. At the whole-leaf level, the phenotype was also synergistic, leading to a shorter and narrower leaf.

Double mutants were also made for *Lgn-R* and *lg2-R* in a mixed genetic background. In *lg2-R* mutants, ligule and auricle are found only at the margins of the leaf with a complete lack of blade sheath boundary over the midrib (Fig. 4D). In the double mutant, leaves are narrower, the midrib remnant of ligule always found in *Lgn-R*

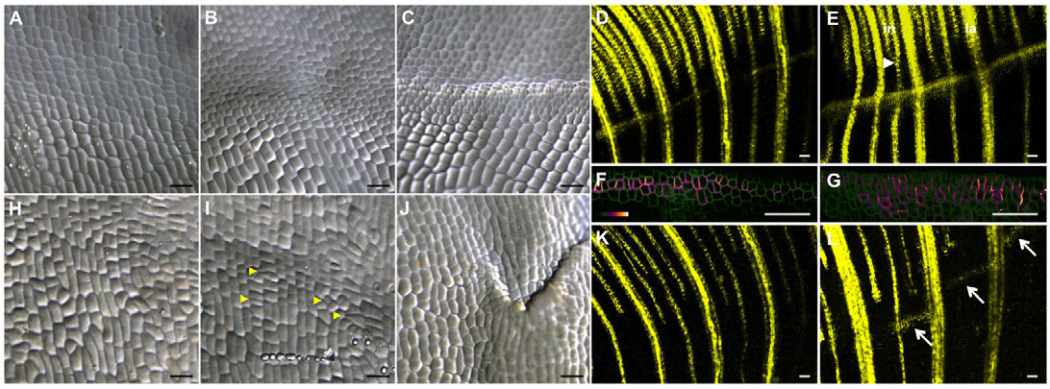

Fig. 3. Preligule development is defective in *Lgn-R*/+. All of the leaves in this figure are presented with midrib towards the right. (**A-C**) Preligular band formation in P5 (A), P6 (B) and P7 (C) leaves of wild-type maize. Anticlinal divisions result in a band of small cells. (**D**,**E**) ZmPIN1a localization (yellow, YFP) is observed at the preligular band of wild-type P6 (D) and P7 (E) leaves. The preligular band is positioned just below the anastomosis zone (arrowhead in E), where the intermediate (in) veins in between the lateral (la) veins merge. (**F**,**G**) Epidermal localization of ZmPIN1a of wild-type P6 (F) and P7 (G) leaves. The color index displays the relative brightness of the signal. Notice that the ZmPIN1a subcellular localization is polarized towards the lateral membranes. (**H-J**) In *Lgn-R*/+, cell divisions occur in P5 (H) and P6 (I) leaves but never form a continuous band. Yellow arrowheads mark some examples of aberrant divisions. P7 (J) leaves show preligule cells developing near the midrib. (**K**,**L**) ZmPIN1a localization in P6 (K) and P7 (L) *Lgn-R*/+ leaves. ZmPIN1a appears in the preligule cells developing near the midrib of *Lgn-R*/+. Anastomosis of intermediate veins is reduced and the epidermal ZmPIN1a expression is not a continuous line (arrows). Scale bars: 100 μm.

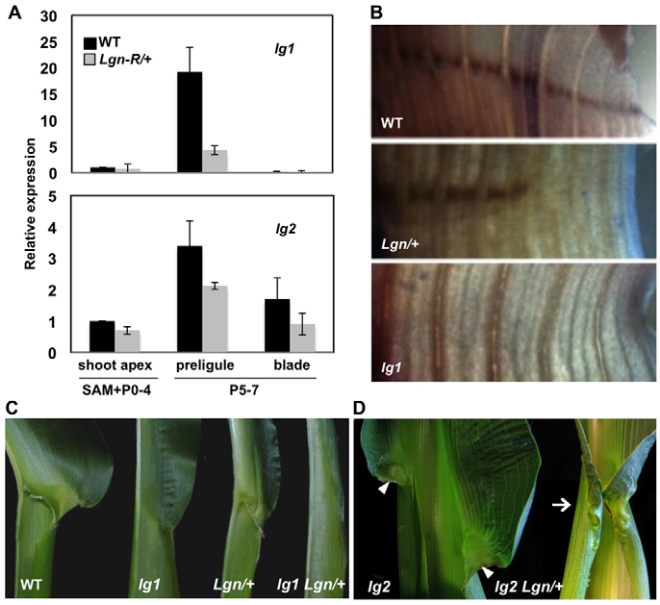

Fig. 4. The interaction of *Lgn-R*/+ with *lg1* and *lg2*.
(**A**) Quantitative RT-PCR results showing *lg1* and *lg2* expression in leaf subdomains of wild-type (black) and *Lgn-R*/+ (gray) maize. *lg1* mRNA accumulates to high levels in the preligule of wild type whereas *lg2* has a broader expression. Both *lg1* and *lg2* are decreased in *Lgn-R*/+. Error bars represent s.d. (**B**) Whole-mount *in situ* hybridization of *lg1* on P7 leaves of wild type, *Lgn-R*/+ and *lg1-R*. Leaves are positioned with midribs towards the left. (**C**) Double mutant phenotype of *lg1-R Lgn-R*/+ in the W23 inbred. Leaves of a normal sibling, *lg1-R*, *Lgn-R*/+ and *lg1-R Lgn-R*/+ are compared (left to right). The double mutant lacks a distinct blade-sheath boundary and appears narrower than both single mutants. (**D**) Double mutant phenotype of *lg2-R Lgn-R*/+. *lg2-R* leaf is compared with *lg2-R Lgn-R*/+. Arrowheads point to the asymmetric marginal ligule and auricle in *lg2-R* compared with the symmetric margins in the double mutant (arrow).

is missing and the margin auricles found in *lg2-R* are greatly reduced. The margin auricle tissue is more symmetrical in the double mutant than *lg2-R* alone, perhaps because the leaf is narrower (Fig. 4D). The synergism in the double mutants suggests that these components interact in setting up the ligule and auricle.

LGN maps to a grass-specific kinase

A mapping population of 2800 chromosomes was used to place *lgn* in a 0.1 cM interval on maize chromosomal bin 9.03. This interval corresponds to 12 Mb of the genome, suggesting that recombination is greatly suppressed in the region owing to proximity to the centromere. Among the 80 genes predicted in this interval, we sequenced cDNAs of the likely candidate genes and found a lesion in a predicted serine/threonine kinase (GRMZM2G134382). Consistent with lesions induced by EMS, we found a G-to-A transition mutation in *Lgn-R* leading to a missense substitution of alanine to threonine at the amino acid level (Fig. 5A,B). In addition, whole-genome sequencing of a pool of 700 *Lgn-R* plants revealed no additional candidate mutations in the mapped interval (see Materials and methods). This kinase was broadly expressed, including shoot apices, tassels, ears and different domains of immature leaves (supplementary material Fig. S3), consistent with the pleiotropic defects observed during development. Expression remained unchanged in the *Lgn-R* mutants (supplementary material Fig. S3).

We looked for independently isolated alleles to confirm that the kinase is encoded by *lgn*. An insertion of the *Activator* (*Ac*) element was found in a collection of insertion lines generated by transposition of *Ac* from the *waxy-m7(Ac)* mutable allele (Cowperthwaite et al., 2002). *Ac* is an autonomous transposon and preferentially transposes to linked sites in the genome (Kunze et al., 1987; McClintock, 1951). The *Ac* insertion of *tac905.29* and an 8-bp duplication resides in the 5′UTR of the kinase, −188 bp upstream of the predicted translation initiation site, and downstream of an in-frame AUG that is transcribed (Fig. 5A). GRMZM2G134382 expression was absent in *tac905.29* (Fig. 5C); however, homozygous *tac905.29* plants have no mutant phenotype (Fig. 5D, left).

In order to isolate additional alleles through germinal transposition events of *Ac*, *tac905.29* was outcrossed, self-pollinated and analyzed in the next generation. A few of the plants displayed a weak phenotype similar to the heterozygous *Lgn-R*, with narrow leaves and reduced auricles (Fig. 5D, middle). Through PCR-based genotyping and sequencing, those plants were determined to be heterozygous for the *Ac* insertion and carry a new allele resulting from *Ac* excision, referred to as *Lgn-dAc*. The excision site retained the 8-bp duplication with a 2-bp sequence difference (Fig. 5A). This *Ac* footprint results in a frameshift that would truncate translation products that initiate from the upstream AUG. Additional outcrosses to B73 and self-pollination produced plants that were homozygous for *Lgn-dAc*. Expression levels were restored to that of wild type (Fig. 5C). Leaves of these plants showed abnormal ligule structures (Fig. 5D, right) and the overall phenotype resembled homozygous *Lgn-R*, with plants failing to thrive.

The *lgn* gene consists of six exons that are predicted to encode a 414 amino acid membrane-associated kinase (Fig. 5A,B). The protein carries a 24 amino acid transmembrane domain and the kinase domain. Along with the kinase domain, LGN contains all 11 subdomains of a typical protein kinase. The invariant amino acids that define the catalytic domain are also conserved (Fig. 5B).

The Ala-to-Thr (A138T) substitution in *Lgn-R* occurs at a highly conserved residue (Fig. 5B, asterisk). In order to determine the effect of the mutation on kinase activity, the mutant version of the kinase domain was expressed and activity was compared with wild type (Fig. 5E). Autophosphorylation activity was greatly reduced in LGN [A138T], suggesting that the *Lgn-R* phenotype results from partial loss of its kinase activity. This result suggests that *Lgn-R* is an antimorph and the reduced kinase activity affects interacting partners whereas loss of the kinase altogether in the *tac905.29* homozygotes does not have a negative consequence. In *Lgn-dAc*, kinase activity is not likely to be affected. We suspect that translation occurs from the upstream AUG and the truncated polypeptide due to the footprint is the cause of the defect.

Paralog expression is upregulated in *Lgn-R*

A paralog of the *lgn* gene was found on chromosome 5 (GRMZM2G009506) and named *sister of liguleless narrow* (*sln*). LGN and SLN are 69.4% identical at the protein level. Orthologs for both LGN and SLN were not found in eudicots or monocots outside of the grass clade, indicating that these are likely to be grass-specific proteins (Fig. 5B). Phylogenetic analysis of the LGN homologs in maize, rice, *Sorghum* and *Brachypodium* showed that LGN was more closely related to its orthologs in other grasses than to any of the SLN orthologs (Fig. 5F). This result indicates that the gene duplication event occurred before speciation among these grasses.

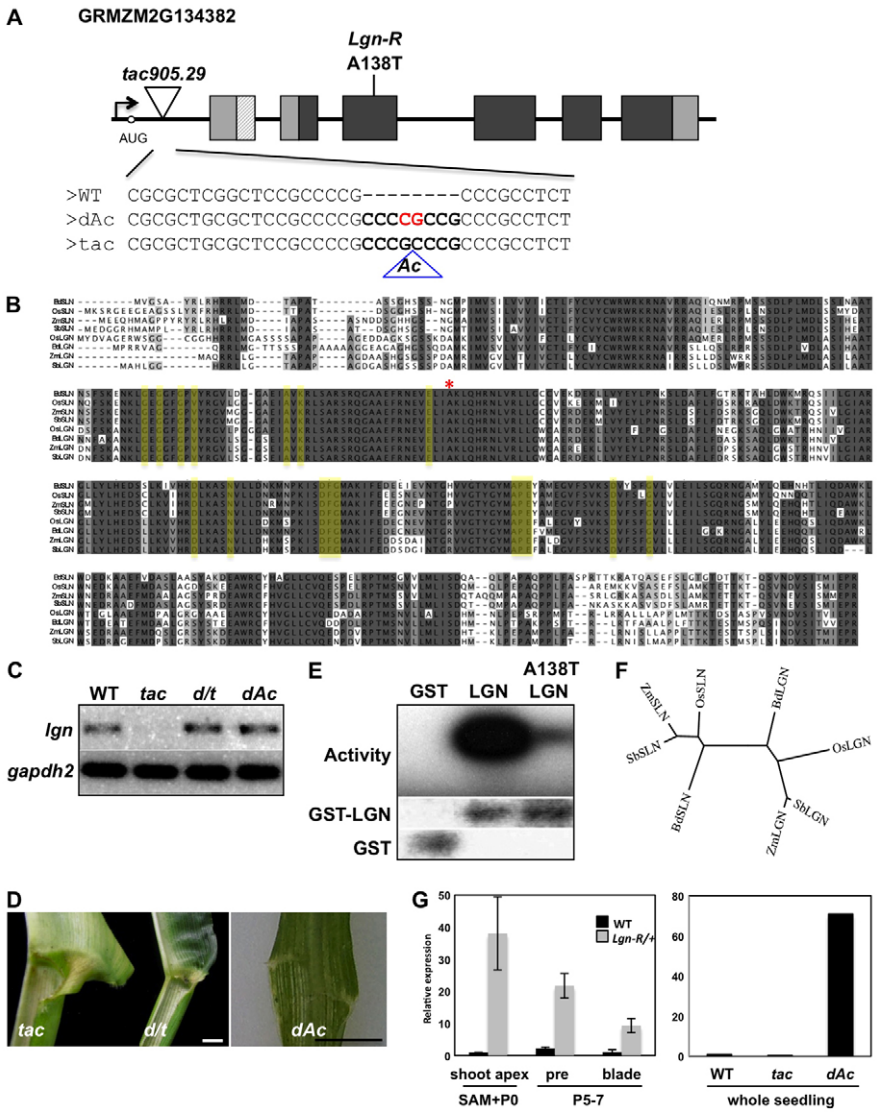

Fig. 5. *lgn* encodes a grass-specific Ser/Thr kinase. (**A**) Schematic of *lgn* genomic region. The 5′UTR, transmembrane domain (striped) and kinase domain (dark gray) are shown. Position of the *Lgn-R* lesion and the *Ac* insertion site are shown. Sequence alignment shows the 8-bp footprint (in bold) resulting from the *Ac* insertion (blue triangle) in *tac905.29* and the change in this sequence (in red) due to the excision of *Ac* in *Lgn-dAc*. The position of an upstream AUG is marked as a white circle. (**B**) Sequence alignment of LGN and SLN to the orthologs in rice, *Brachypodium* and *Sorghum*. Invariant amino acids of the kinase domain are in yellow. The *Lgn-R* mutation is indicated as a red asterisk. (**C**) Semi-quantitative RT-PCR showing *lgn* expression in W22, *tac905.29* homozygote (*tac*), *Lgn-dAc/tac905.29* (*d/t*) and *Lgn-dAc* homozygote (*dAc*). *lgn* expression is abolished in *tac905.29* but not affected in *Lgn-dAc/tac905.29* or *Lgn-dAc*. (**D**) Phenotype of *Lgn-dAc/tac905.29* and *Lgn-dAc* compared with *tac905.29* on left. *Lgn-dAc/tac905.29* leaves are narrower than wild type and the blade-sheath boundary shows a smaller auricle. The phenotype is more severe in *Lgn-dAc/Lgn-dAc*, which resembles *Lgn-R* homozygotes. Scale bars: 1 cm. (**E**) Autophosphorylation assay of LGN and LGN[A138T]. The kinase activity of LGN is greatly reduced in the mutant. Gel staining are shown for loading controls of GST, GST-LGN and GST-LGN[A138T]. (**F**) Phylogenetic tree based on the alignment in B shows that LGN is more closely related to its orthologs in rice, *Brachypodium* and *Sorghum* than to SLN. (**G**) Quantitative RT-PCR showing upregulation of *sln* in *Lgn-R*/+ (gray) compared with B73 (black) in all leaf subdomains ($P<0.005$) and in *Lgn-dAc* seedlings. Error bars represent s.d.

sln mRNA was barely detectable in leaf tissues of wild type and *tac905.29* homozygotes. However, it was greatly increased in all leaf subdomains of *Lgn-R* heterozygotes and in *Lgn-dAc* homozygous plants (Fig. 5G). Thus, the expression of *sln* appears to be an important and unifying component of the *Lgn* phenotype.

DISCUSSION

The semi-dominant *Lgn-R* mutant displays narrower and shorter leaves with a defective ligule and auricle. *Lgn-R* heterozygotes also have fewer tassel branches and some lack ears altogether, although phenotypic severity of the heterozygote varies with inbred. Defects are more severe in homozygotes, as the plants fail to proceed to reproductive development. The ligule defect initiates early in leaf development with reduced *lg1* and *lg2* expression and altered ZmPIN1a expression. *lgn* maps to a grass-specific kinase. Although an *Ac* insertion in the 5′UTR of the gene has no obvious phenotype, an *Ac* excision derivative that leaves a footprint has a *Lgn* phenotype. In further support of the kinase as the gene, kinase activity is reduced in *Lgn-R* mutants and expression of its paralog, *sln*, is greatly increased in both *Lgn-R* and *Lgn-dAc*.

The nature of the *Lgn* mutation

The *Lgn-R* mutation leads to a decrease in its kinase activity. If LGN was the only component in this signal transduction pathway, the *tac905.29* homozygote might also show a similar phenotype owing to the absence of protein. However, the plants appear normal, suggesting that additional factors exist in the pathway to compensate for the absence of *lgn* in the *tac905.29* allele. By contrast, the phosphorylation-defective protein encoded by *Lgn-R* might poison a complex that includes SLN or a common partner of both LGN and SLN. A similar result is seen in *clv1* mutants, in which dominant-negative alleles of a gene have a more severe phenotype compared with null alleles (Diévart et al., 2003).

How the footprint in the 5′UTR of the *Lgn-dAc* allele leads to a phenotype is unknown. Mutations have been documented due to changes in 5′UTR sequences that affect gene regulation (Pippucci et al., 2011; Wethmar et al., 2010); however, *lgn* transcript levels are not changed in *Lgn-dAc*. Another alternative is that translation begins from the upstream AUG. If this were the case, then the footprint results in a truncated polypeptide. Either this short polypeptide interferes with normal LGN function or its presence leads to translational skipping of the predicted AUG (Chua et al., 2012). Regardless of the mechanism, the increase in *sln* expression

in both *Lgn* mutants suggests a crucial role for functional LGN in negative feedback regulation of *sln* expression. Failure to block the accumulation of *sln* might be at the root of the *Lgn* defect, leading to the pleiotropic defects throughout development. If this model is correct, then a loss of function *sln* mutant would correct the *Lgn-R* and *Lgn-dAc* defects.

Revisiting the ligule pathway

Ligule development occurs early in maize leaf development (Fig. 6A). An inductive signal (the 'preligule signal') is thought to propagate from the midrib to the margin to initiate a localized increase in longitudinal and transverse anticlinal divisions in competent cells (Becraft and Freeling, 1991; Foster et al., 2004; Harper and Freeling, 1996). These divisions progress towards the margins of the leaf, forming a band of small cells called the preligular band, which separates the cells that will differentiate into blade from those that will differentiate into sheath (Fig. 3A-C) (Fowler and Freeling, 1996). The signal perception and propagation needed to establish the boundary zone and initiate a ligule involve LG1 and LG2 (Becraft and Freeling, 1991; Becraft et al., 1990; Harper and Freeling, 1996; Moreno et al., 1997; Sylvester et al., 1990; Walsh et al., 1998). Both *lg1* and *lg2* transcripts are reduced in *Lgn-R* mutants, and double mutants of *Lgn-R* with either *lg1-R* or *lg2-R* are synergistic (Fig. 4). We hypothesize that LGN and SLN function as signaling components in this pathway.

RNA expression as well as mutant phenotypes suggest that LG2 and LGN function early in establishing the position of the ligule. *lg2* mutants lack a blade-sheath boundary at the midrib, but the margins recover (Fig. 6B). Preligule cell divisions do not occur at the midrib region (Walsh et al., 1998), indicating that neither is the boundary established in these cells nor are cells receptive to a signal. The ligules at the margin suggest that other factors are responsible for this recovery. Indeed, all ligule and auricle disappear in a *lg1-R lg2-R* double mutant (Harper and Freeling, 1996). The displaced ligules at the margins support an early role for LG2 in coordinating the boundary position from the center of the leaf outward. *Lgn-R* has a functional ligule over the midrib, indicating proper boundary initiation (Fig. 6C). The lack of distinct blade-sheath boundary towards the margins suggests that LGN functions in perceiving or transmitting the signal for boundary establishment outside of the midrib region. LG1 is thought to function later in the pathway during preligule cell division. Transverse divisions of the preligule band occur in *lg1* mutants, but longitudinal and periclinal divisions do not (Fig. 6D) (Becraft et al., 1990). The lack of any blade-sheath boundary in *lg1-R Lgn-R* double mutants, however, suggests that LG1 might also play a redundant role with LGN in establishing the position of the ligule.

In wild-type leaves, development of the preligular band is coincident with subcellular localization of the auxin transporter ZmPIN1a (Fig. 3D-G). The preligule epidermal localization occurs at lateral membranes, which is perpendicular to that of vascular ZmPIN1a at the position of intermediate vein anastomosis. Early studies have shown that intermediate veins initiate from the tip of late P3 to early P4 leaves and differentiate basipetally (Sharman, 1942). At P7 to P8, the veins anastomose and only one intermediate vein enters the presumptive sheath. In *Lgn-R* leaves, epidermal ZmPIN1a is observed in patches of cells adjacent to the midvein in a discontinuous pattern (Fig. 3L). The localization expands into a short band of cells, which seems to initiate from the lateral vein towards the margin. These observations support the hypothesis that LGN plays a role in establishment of the boundary zone and that the defective allele has interfered with its normal function.

Previous models proposed that a preligule signal initiates near the midrib and travels towards the leaf margins. Our data reveal that auxin and LGN are two new components in establishment of the ligule position and its propagation. Our data also suggest that the signal is discontinuous along the medial-lateral axis and forms from large veins, which become connected as the signals meet in between the veins (Fig. 6A). How this flow of auxin integrates with *lg1*, *lg2* and *lgn* in establishing the preligular band requires further investigation.

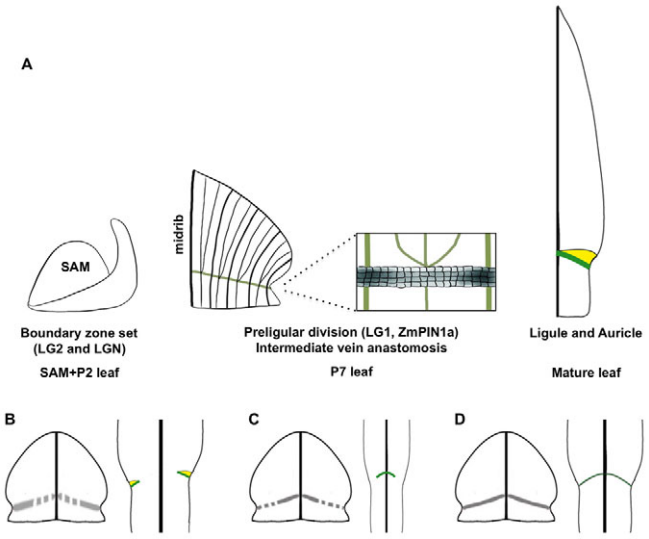

Fig. 6. Model for ligule development in maize. (**A**) LGN and LG2 establish the position of the boundary zone at the base of a developing leaf. At the boundary zone of a P7 leaf, epidermal cells divide rapidly to form a continuous preligule band, which is marked by ZmPIN1a expression. LG1 is required for proper division to occur. In a mature leaf, the ligule (green) and auricle (yellow) separate blade from sheath cells. (**B**) In *lg2-R*, the blade-sheath boundary fails at the midrib owing to the absence of LG2. Recovery of ligule and auricle occur at the margin but is displaced. (**C**) In *Lgn-R*, preligular signals initiate normally, but without a functional LGN, signal transmission fails. As a result, the ligule only appears near the midrib. (**D**) In *lg1-R*, signal initiation and transmission occur normally, setting up a blade-sheath boundary. Longitudinal anticlinal and periclinal divisions fail, however, preventing ligule outgrowth.

Coordination of leaf width and preligule establishment

The narrow leaf phenotype of *Lgn-R* suggests the involvement of LGN in leaf expansion. Previous studies of maize mutants with narrow leaves suggest that different domains exist along the medial-lateral axis of the maize leaf. The leaves of *narrow sheath* (*ns*) mutants are half the width of normal siblings but have normal ligule and auricles (Scanlon et al., 1996). The *ns* defect removes the marginal domain of the leaf, resulting in a blunt-edged leaf (Scanlon et al., 1996; Scanlon and Freeling, 1997). The dominant mutant *Wavy auricle in blade1* (*Wab1*) also has narrow leaves, but its leaf margins are tapered, as in wild type, and double mutants with *ns* are additive (Hay and Hake, 2004). *Wab1* homozygotes lack a ligule in a domain internal to the marginal domain, suggesting that *Wab1* has failed to elaborate or expand this domain. Similar to *Wab1*, *Lgn-R* leaves have a tapered margin, suggesting that the *Lgn-R* defect also occurs inside the marginal domain. In

addition, *Wab1* is synergistic with *lg1* (Foster et al., 2004). A difference between *Wab1* and *Lgn-R* is that *Wab1* overexpresses *lg1* and recovers auricle and ligule at the very margin, whereas *Lgn-R* does the opposite. These comparisons suggest that signals required to establish the position of the ligule are coordinated with signals that operate internal to the marginal domains to promote leaf width expansion. Future studies with LGN will be aimed at identifying the signals involved in the cell-cell communication.

Acknowledgements
We thank M. G. Neuffer for the *Lgn-R* mutation, Nathalie Bolduc for help with the genomic DNA library preparation, and Devin O'Connor for help with confocal imaging. We are grateful to Michael Lewis and the other members of the Hake lab for their continual input and ideas, and David Hantz and his crew for running the greenhouse.

Funding
This work was supported by the National Science Foundation (NSF) [MCB1052051]; and the United States Department of Agriculture Agricultural Research Service (USDA-ARS).

Competing interests statement
The authors declare no competing financial interests.

Supplementary material
Supplementary material available online at
http://dev.biologists.org/lookup/suppl/doi:10.1242/dev.085787/-/DC1

References

Becraft, P. W. and Freeling, M. (1991). Sectors of liguleless-1 tissue interrupt an inductive signal during maize leaf development. *Plant Cell* **3**, 801-807.
Becraft, P. W., Bongard-Pierce, D. K., Sylvester, A. W., Poethig, R. S. and Freeling, M. (1990). The liguleless-1 gene acts tissue specifically in maize leaf development. *Dev. Biol.* **141**, 220-232.
Candela, H. and Hake, S. (2008). The art and design of genetic screens: maize. *Nat. Rev. Genet.* **9**, 192-203.
Carraro, N., Forestan, C., Canova, S., Traas, J. and Varotto, S. (2006). ZmPIN1a and ZmPIN1b encode two novel putative candidates for polar auxin transport and plant architecture determination of maize. *Plant Physiol.* **142**, 254-264.
Chua, J. J. E., Schob, C., Rehbein, M., Gkogkas, C. G., Richter, D. and Kindler, S. (2012). Synthesis of two SAPAP3 isoforms from a single mRNA is mediated via alternative translational initiation. *Sci. Rep.* **2**, doi:10.1038/srep00484.
Chuck, G., Muszynski, M., Kellogg, E., Hake, S. and Schmidt, R. J. (2002). The control of spikelet meristem identity by the branched silkless1 gene in maize. *Science* **298**, 1238-1241.
Cowperthwaite, M., Park, W., Xu, Z., Yan, X., Maurais, S. C. and Dooner, H. K. (2002). Use of the transposon Ac as a gene-searching engine in the maize genome. *Plant Cell* **14**, 713-726.
Dereeper, A., Guignon, V., Blanc, G., Audic, S., Buffet, S., Chevenet, F., Dufayard, J. F., Guindon, S., Lefort, V., Lescot, M. et al. (2008). Phylogeny.fr: robust phylogenetic analysis for the non-specialist. *Nucleic Acids Res.* **36**, W465-W469.
Diévart, A., Dalal, M., Tax, F. E., Lacey, A. D., Huttly, A., Li, J. and Clark, S. E. (2003). CLAVATA1 dominant-negative alleles reveal functional overlap between multiple receptor kinases that regulate meristem and organ development. *Plant Cell* **15**, 1198-1211.
Edgar, R. C. (2004). MUSCLE: multiple sequence alignment with high accuracy and high throughput. *Nucleic Acids Res.* **32**, 1792-1797.
Eshed, Y., Baum, S. F., Perea, J. V. and Bowman, J. L. (2001). Establishment of polarity in lateral organs of plants. *Curr. Biol.* **11**, 1251-1260.
Foster, T., Hay, A., Johnston, R. and Hake, S. (2004). The establishment of axial patterning in the maize leaf. *Development* **131**, 3921-3929.
Fowler, J. E. and Freeling, M. (1996). Genetic analysis of mutations that alter cell fates in maize leaves: dominant Liguleless mutations. *Dev. Genet.* **18**, 198-222.
Gallavotti, A., Yang, Y., Schmidt, R. J. and Jackson, D. (2008). The Relationship between auxin transport and maize branching. *Plant Physiol.* **147**, 1913-1923.
Gälweiler, L., Guan, C., Müller, A., Wisman, E., Mendgen, K., Yephremov, A. and Palme, K. (1998). Regulation of polar auxin transport by AtPIN1 in Arabidopsis vascular tissue. *Science* **282**, 2226-2230.
Harper, L. and Freeling, M. (1996). Interactions of liguleless1 and liguleless2 function during ligule induction in maize. *Genetics* **144**, 1871-1882.
Hay, A. and Hake, S. (2004). The dominant mutant Wavy auricle in blade1 disrupts patterning in a lateral domain of the maize leaf. *Plant Physiol.* **135**, 300-308.
Kunze, R., Stochaj, U., Laufs, J. and Starlinger, P. (1987). Transcription of transposable element Activator (Ac) of Zea mays L. *EMBO J.* **6**, 1555-1563.
Langmead, B., Trapnell, C., Pop, M. and Salzberg, S. L. (2009). Ultrafast and memory-efficient alignment of short DNA sequences to the human genome. *Genome Biol.* **10**, R25.
Li, H., Handsaker, B., Wysoker, A., Fennell, T., Ruan, J., Homer, N., Marth, G., Abecasis, G., Durbin, R. and 1000 Genome Project Data Processing Subgroup (2009). The Sequence Alignment/Map format and SAMtools. *Bioinformatics* **25**, 2078-2079.
McClintock, B. (1951). Chromosome organization and genic expression. *Cold Spring Harb. Symp. Quant. Biol.* **16**, 13-47.
Michelmore, R. W., Paran, I. and Kesseli, R. V. (1991). Identification of markers linked to disease-resistance genes by bulked segregant analysis: a rapid method to detect markers in specific genomic regions by using segregating populations. *Proc. Natl. Acad. Sci. USA* **88**, 9828-9832.
Moon, J. and Hake, S. (2011). How a leaf gets its shape. *Curr. Opin. Plant Biol.* **14**, 24-30.
Moreno, M. A., Harper, L. C., Krueger, R. W., Dellaporta, S. L. and Freeling, M. (1997). liguleless1 encodes a nuclear-localized protein required for induction of ligules and auricles during maize leaf organogenesis. *Genes Dev.* **11**, 616-628.
Neuffer, M. G., Johal, G., Chang, M. T. and Hake, S. (2009). Mutagenesis – the key to genetic analysis. In *Handbook of Maize: Its Biology* (ed. J. L. Bennetzen and S. Hake), pp. 63. New York, NY: Springer.
Ossowski, S., Schneeberger, K., Clark, R. M., Lanz, C., Warthmann, N. and Weigel, D. (2008). Sequencing of natural strains of Arabidopsis thaliana with short reads. *Genome Res.* **18**, 2024-2033.
Pippucci, T., Savoia, A., Perrotta, S., Pujol-Moix, N., Noris, P., Castegnaro, G., Pecci, A., Gnan, C., Punzo, F., Marconi, C. et al. (2011). Mutations in the 5′ UTR of ANKRD26, the ankirin repeat domain 26 gene, cause an autosomal-dominant form of inherited thrombocytopenia, THC2. *Am. J. Hum. Genet.* **88**, 115-120.
Robinson, J. T., Thorvaldsdóttir, H., Winckler, W., Guttman, M., Lander, E. S., Getz, G. and Mesirov, J. P. (2011). Integrative genomics viewer. *Nat. Biotechnol.* **29**, 24-26.
Scanlon, M. J. and Freeling, M. (1997). Clonal sectors reveal that a specific meristematic domain is not utilized in the maize mutant narrow sheath. *Dev. Biol.* **182**, 52-66.
Scanlon, M. J., Schneeberger, R. G. and Freeling, M. (1996). The maize mutant narrow sheath fails to establish leaf margin identity in a meristematic domain. *Development* **122**, 1683-1691.
Schmidt, R. J., Ketudat, M., Aukerman, M. J. and Hoschek, G. (1992). Opaque-2 is a transcriptional activator that recognizes a specific target site in 22-kD zein genes. *Plant Cell* **4**, 689-700.
Sharman, B. C. (1942). Developmental anatomy of the shoot of *Zea mays* L. *Ann. Bot. (Lond.)* **6**, 245-282.
Sylvester, A. W., Cande, W. Z. and Freeling, M. (1990). Division and differentiation during normal and liguleless-1 maize leaf development. *Development* **110**, 985-1000.
Walsh, J., Waters, C. A. and Freeling, M. (1998). The maize gene liguleless2 encodes a basic leucine zipper protein involved in the establishment of the leaf blade-sheath boundary. *Genes Dev.* **12**, 208-218.
Wethmar, K., Smink, J. J. and Leutz, A. (2010). Upstream open reading frames: molecular switches in (patho)physiology. *BioEssays* **32**, 885-893.

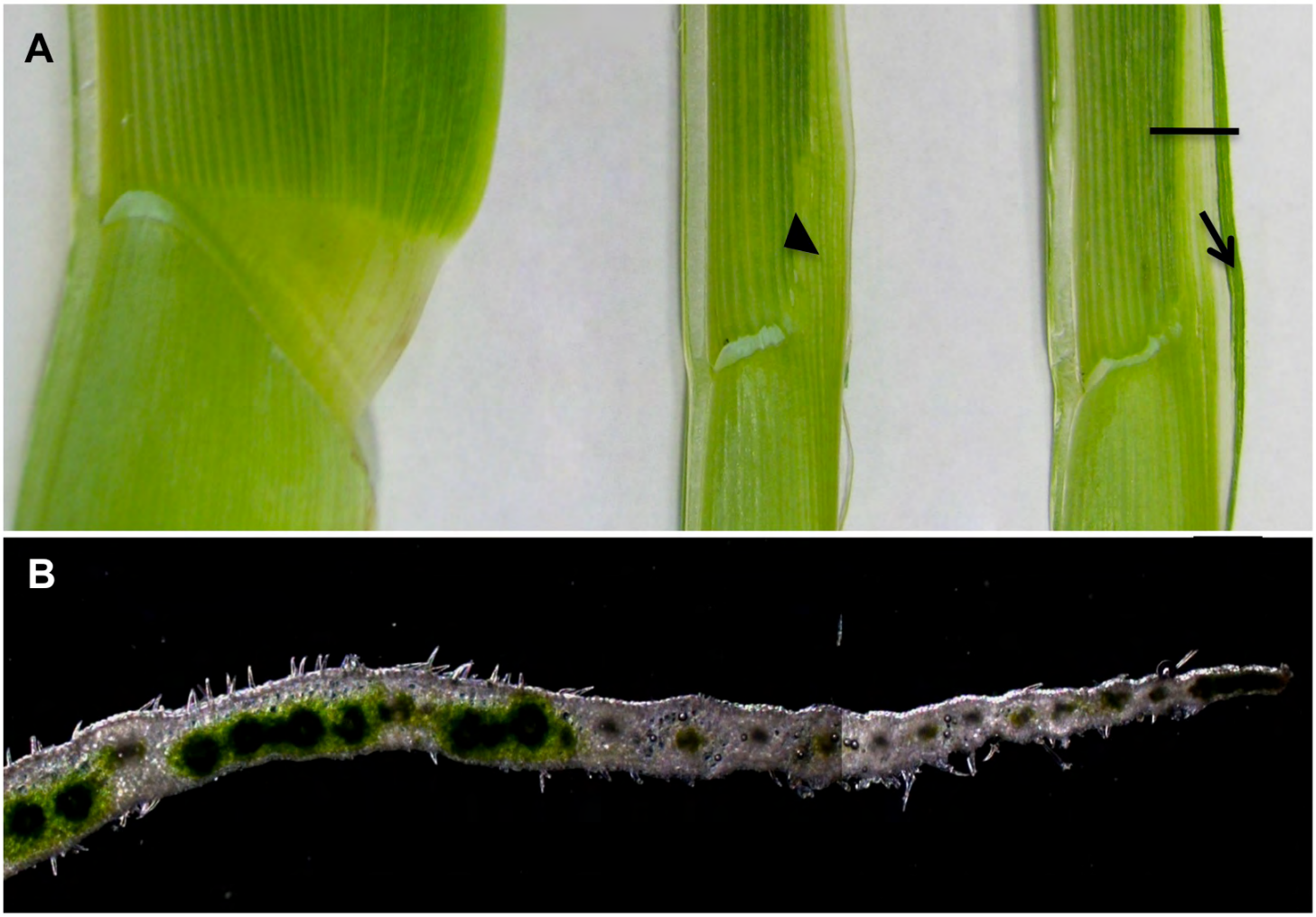

Fig. S1. Marginal boundary is disrupted in *Lgn-R*. (**A**) A wild-type leaf (left) compared with *Lgn-R*/+ leaves. Sheath tissue extends into the blade (arrowhead) or blade tissue invades the sheath (arrow) indicating that the blade-sheath boundary in not established properly at this region**.** (**B**) Cross section of the area marked in A.

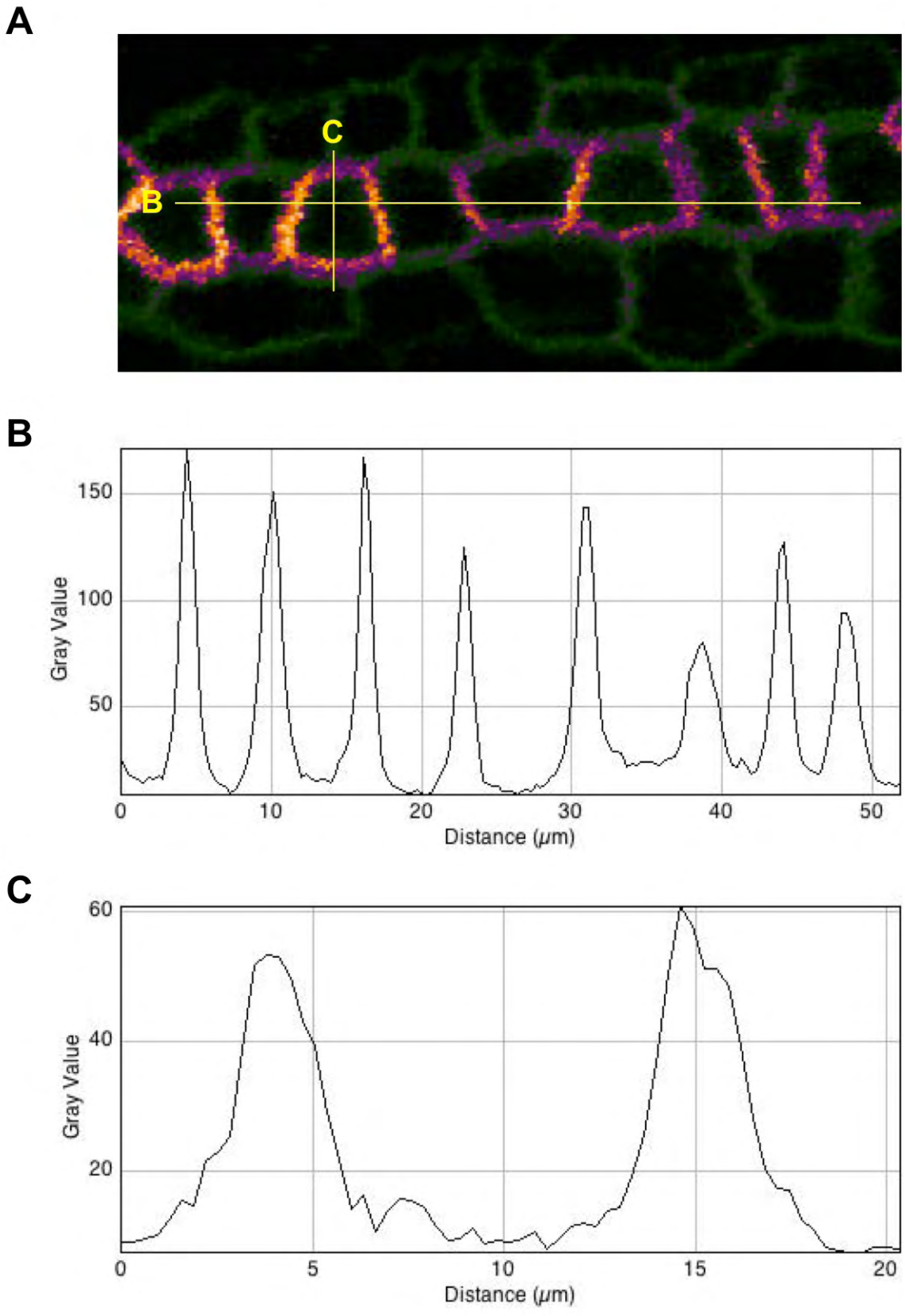

Fig. S2. ZmPIN1a is localized to the lateral membranes of the preligule cells. (**A**) Epidermal expression of the ZmPIN1a at the preligular band. The yellow lines indicate the axes along which analysis was carried out (shown in B and C). (**B**) The image shown in A was processed with ImageJ to calculate the intensity of ZmPIN1a along the median-lateral axis. (**C**) Representative plot of the intensity of ZmPIN1a along the proximal-distal axis. The *y*-axis shows the intensity of the signal. Comparing the intensity in B and C indicates that ZmPIN1a is polarized towards the lateral membranes.

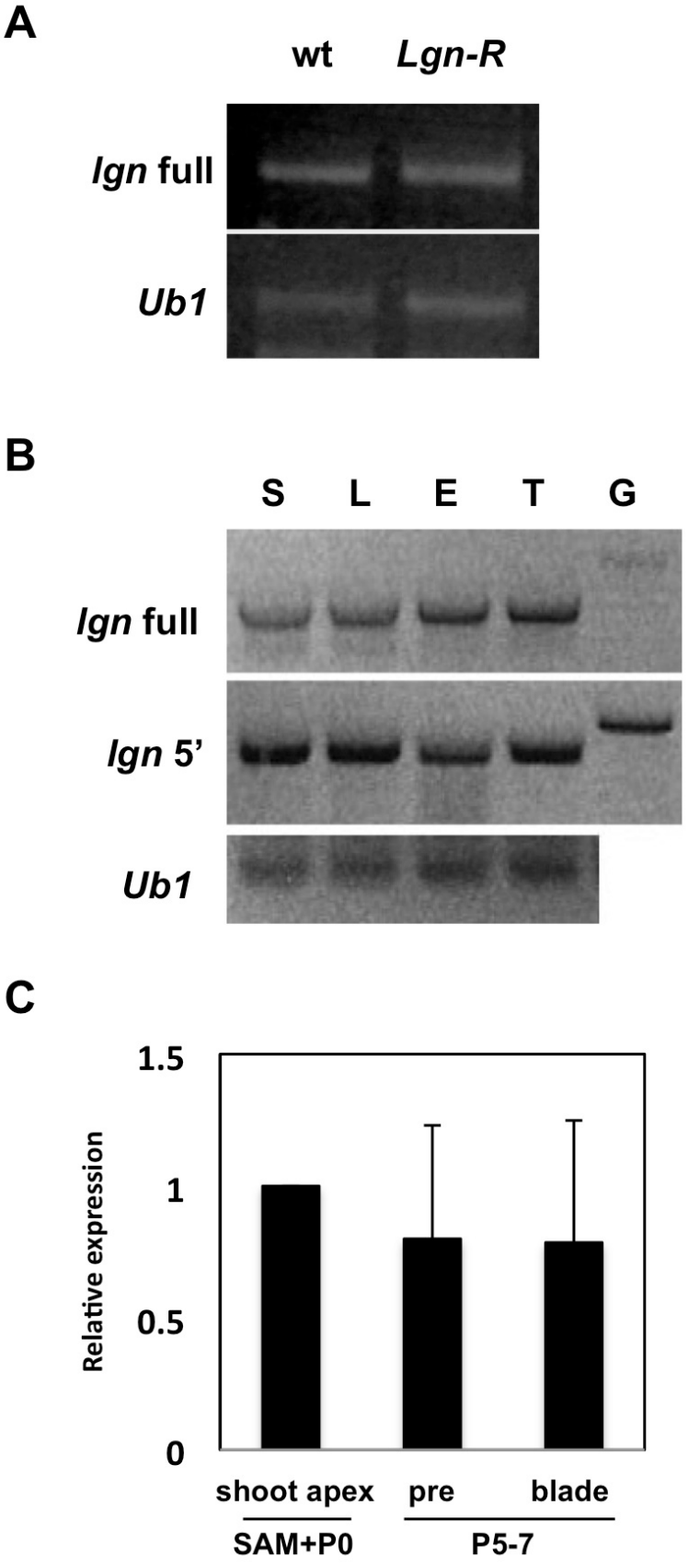

Fig. S3. *lgn* is broadly expressed during development. (**A**) *lgn* expression remains unchanged in *Lgn-R*. (**B**) *lgn* is expressed in various tissues. S, SAM; L, immature leaves; E, immature ears; T, immature tassels; G, genomic DNA. (**C**) *lgn* is expressed in different leaf domains.